

Enhanced intraband carrier relaxation in quantum dots due to the effect of plasmon–LO-phonon density of states in doped heterostructures

A. V. Fedorov,* A. V. Baranov, and I. D. Rukhlenko

S. I. Vavilov State Optical Institute, 12 Birzhevaya Liniya 199034 St. Petersburg, Russia

S. V. Gaponenko

Institute of Molecular and Atomic Physics, National Academy of Belarus 220072, Minsk, Belarus

(Received 18 June 2004; revised manuscript received 21 January 2005; published 9 May 2005)

The effect of surface plasmon–LO-phonon excitations of the doped elements of heterostructures in the electronic dynamics of quantum dots has been theoretically studied in a double heterostructure. It has been found that, in contrast to a single heterostructure, critical points can arise in the surface plasmon–LO-phonon density of states for layered structures. This results in enhanced quantum-dot intraband carrier relaxation as compared with the single heterostructure. It has been shown that the relaxation rates and spectral positions of relaxation windows strongly depend on the thickness of the layer containing the quantum dots. These effects of the critical points of density of states have been demonstrated using a model n-GaAs/GaAs/air heterostructure with an InAs quantum dot embedded in the GaAs layer.

DOI: 10.1103/PhysRevB.71.195310

PACS number(s): 78.66.Fd, 63.22.+m, 71.35.Cc, 78.55.Cr

I. INTRODUCTION

The problem of energy and phase relaxation in quantum dots (QDs) is of great interest not only for fundamental physics, but it also becomes increasingly important for nanoelectronic applications. The creation of high-quality single-electron transistors,¹ logic elements (quantum bits),² memory cells,³ and lasers⁴ based on quantum-dot heterostructures requires detailed information on the relaxation parameters of the systems in question. This problem is especially important because nanoelectronic devices should be incorporated into large integral circuits with closely packed structural elements. Recent estimations allow one to expect that the characteristic distances between the elements of the integral circuits will fall within the range of several tens of nanometers. It is believed that the 22 nm logic technology will be used to fabricate high-performance microprocessors and static random access memory (SRAM) chips at the close of the decade. That is why the questions as to the mutual influence of the nanoelectronic devices and how they are affected by the metallic and doped semiconductor components of the heterostructures and integral circuits (interconnectors, contacts, substrates, buffer layers, etc.) become topical. Therefore, studies on the interactions with characteristic distances of several tens of nanometers, which induce energy and phase relaxation processes in QDs, are of great importance.

In recent years much attention in this field has been paid to the relaxation processes caused by interactions with different elementary excitations localized inside a quantum dot or at its interface. The effects of confined and interface optical phonons^{5–10} and plasmons^{11–13} on the QD electronic dynamics have been investigated. Multiphonon mediated intraband relaxation processes involving longitudinal optical (LO) and acoustic phonons have been studied.^{8,10,14,15} A defect-assisted multiphonon emission mechanism^{16–18} has been suggested to explain the fast carrier relaxation in quantum dots. Important theoretical^{6,19} and experimental²⁰ data

concerning energy relaxation have been obtained in studies of the polaronlike states in QDs. In this case the energy relaxation results from the crystal anharmonicity which determines the finite lifetime of the optical phonons involved in the polarons. The Auger-like process^{21,22} is considered as another effective mechanism of intraband carrier relaxation.

Since actual QD-based devices are complicated heterostructures composed of many components (e.g., the host matrix, quantum wells and wires, capping, buffer, and wetting layers, etc.), several studies on the QD electronic dynamics affected by interactions with the environmental elementary excitations have been performed. The interaction between the QD electronic subsystem and the barrier and/or matrix optical and acoustical phonons^{7,8,23–25} has been investigated. The influence of the nearest surroundings on the QD dynamics has been studied in some works. For example, the homogeneous broadening of optical transitions in self-assembled quantum dots caused by the elastic Coulomb collisions between carriers in the wetting layer and in the dots²⁶ has been analyzed. The QD electronic dephasing caused by charge fluctuations in the impurity state due to its recharging through the free electron reservoir² has been investigated. On the other hand, not only the environmental free charges, but also the plasmons and plasmon phonons, which reside in doped heterostructure components, will interact with the QD electronic subsystem. It is clear that the QD carriers will strongly interact with environmental excitations accompanied by the electric fields at close contact of the dots with the doped components. These components, e.g., doped substrates, are often located several tens of nanometers away from the quantum dots. Even so, the QD electronic subsystem can be strongly coupled with plasmons or plasmon phonons of the doped substrate. This coupling results in new intraband relaxation mechanisms in the QDs. This type of relaxation process involving the bulk and surface plasmon–LO phonons has been studied in some works.^{27,28} It has been shown that the QD intraband carrier relaxation with

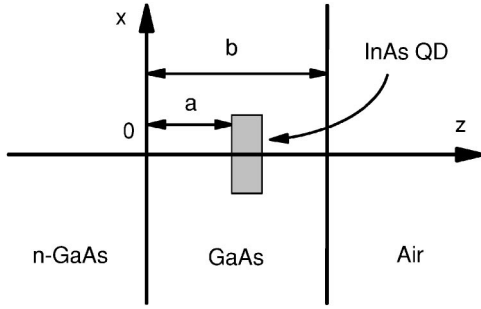


FIG. 1. The double heterostructure considered in the model. b is the thickness of the undoped layer, and a is the distance between the doped semiconductor and the quantum dot.

an emission of the substrate bulk and surface plasmon–LO-phonon modes may be sufficiently effective even if the distance between the QD and the substrate is about 100 nm. If the distance equals several tens of nanometers, then these relaxation mechanisms can be dominant. Since the relaxation rates and the spectral positions of the corresponding relaxation windows are determined by the dispersion of the plasmon–LO-phonon modes, intuition suggests that the relaxation process with the bulk plasmon–LO phonons weakly depends on the heterostructure design. On the other hand, one would expect that the coupling between the QD electronic subsystem and the substrate surface plasmon–LO phonons is strongly affected by the heterostructure’s architecture. The reason is that the dispersion of the surface plasmon–LO-phonon modes depends on the heterostructure’s arrangement as the polaritonic excitations do.²⁹

In this work we study the influence of the heterostructure’s design on the surface plasmon–LO-phonon dispersion and density of states. We show that critical points can arise in the density of states for layered heterostructures. The existence of the critical points results in an enhancement of the QD intraband carrier relaxation via interaction between the carriers and the electric potential induced by the surface plasmon–LO-phonon (SPLP) modes in the doped elements of heterostructures.

II. THE HYDRODYNAMIC MODEL OF THE SURFACE PLASMON–LO-PHONON EXCITATIONS

In order to demonstrate the important role of the heterostructure’s design in the SPLP excitations and in the coupling between the QD carriers and the SPLP modes let us consider a simple model of a double heterostructure (Fig. 1). The heterostructure is composed of a half space filled with a doped semiconductor with a plane interface and an undoped semiconductor layer with a thickness b . The quantum dot is located at a distance a from the doped material. We will find the SPLP eigenmodes and the electric potential induced by them at the dot position using an approach used earlier^{27,28} for the description of the plasmon–LO-phonon modes in a single heterostructure (e.g., $b \rightarrow \infty$). The quantum dot is considered here as a probe for electric fields induced by the SPLP, and therefore the dot and/or SPLP interaction does not noticeably perturb the SPLP and QD energy spectra.

Our approach is based on the combination of the hydrodynamic model^{30,31} for plasmons and the local dielectric formalism for dispersionless optical phonons. Although the hydrodynamic model has well-known limitations in quantitative analysis,^{32,33} among which it is worth noting that the presumption about a local statistical equilibrium in every point of space and the long-wave limit of the kinetic equation, this macroscopic description of many-electron problems offers some advantages over microscopic descriptions, e.g., random phase approximation, because it allows one to obtain the simple and physically transparent qualitative results concerning the spatially inhomogeneous systems. Particularly the dispersion relation of the SPLP modes and electric field induced by them can be easily calculated. The hydrodynamic model is successfully applied to various kinetic problems^{30–37} that allow us to compare our results and well-known results^{30,31} by means of the consideration of corresponding limiting cases.

The starting point for our consideration of the SPLP excitations is the Bloch equations describing the hydrodynamic motion of electron gas coupled with the electromagnetic and LO-phonon fields,^{27,28}

$$\begin{aligned} \frac{\partial n}{\partial t} &= -\nabla \cdot (n\mathbf{v}), \\ \frac{\partial \mathbf{v}}{\partial t} &= -\mathbf{v} \cdot (\nabla \mathbf{v}) + \frac{e}{m} \nabla \varphi - \frac{1}{m} \nabla \int_0^n \frac{dp(n')}{n'}, \\ \Delta \varphi &= \frac{4\pi e}{\varepsilon_\infty} (n - N_0) + \frac{4\pi\alpha}{\varepsilon_\infty} \nabla \cdot \mathbf{u}, \\ \frac{\partial^2 \mathbf{u}}{\partial t^2} &= -\omega_T^2 \mathbf{u} - \frac{\alpha}{\rho} \nabla \varphi, \end{aligned} \quad (1)$$

where $n(\mathbf{r}, t)$, $p(\mathbf{r}, t)$, and $\mathbf{v}(\mathbf{r}, t)$ are the macroscopic density, pressure, and velocity of the electron gas, m is the effective mass of the free carriers, $\varphi(\mathbf{r}, t)$ is the self-consistent electrostatic potential, N_0 is the impurity density, $\mathbf{u}(\mathbf{r}, t)$ and ρ are the relative displacement and reduced-mass density of the ion pair, $\alpha = \omega_T [(\varepsilon_0 - \varepsilon_\infty)\rho/4\pi]^{1/2}$, ω_T is the frequency of transversal optical phonons at the Brillouin-zone center, and ε_0 and ε_∞ are the low- and high-frequency dielectric constants, respectively. For simplicity’s sake, we neglect the retardation effects and the dispersion of optical phonons. The system (1) becomes complete when the state equation defining the connection between $n(\mathbf{r}, t)$, $p(\mathbf{r}, t)$, and temperature is specified. In general, this connection for electron gas is implicitly determined by the couple of equations,

$$\begin{aligned} n &= \frac{2\sqrt{2}m^{3/2}T^{5/2}}{3\pi^2\hbar^3} \int_0^\infty \frac{dz z^{3/2}}{\exp(z - \mu/T) + 1}, \\ p &= \frac{\sqrt{2}(mT)^{3/2}}{\pi^2\hbar^3} \int_0^\infty \frac{dz z^{1/2}}{\exp(z - \mu/T) + 1}, \end{aligned} \quad (2)$$

where T and μ are the temperature in energy units and the chemical potential, respectively. In the cases of nondegener-

ate and degenerate electron gas, the system (2) is reduced to simple state equations, $p=nT$ and $p=(3\pi^2)^{2/3}\hbar^2n^{5/3}/5m$, respectively. For a strong coupling between LO phonons and plasmons, the closeness of their frequencies is necessary. We restrict our consideration to the second case since the LO-phonon and plasma frequencies are values of the same order of magnitude at an electron concentration of about 10^{18} cm^{-3} , when electron gas is degenerate as a rule. Then, we suppose that the electron gas motion is laminar and can be described by the velocity potential $\psi(\mathbf{r},t)$ according to $\nabla\psi=-\mathbf{v}$. Then Eqs. (1) become

$$\begin{aligned} \frac{\partial n}{\partial t} &= \nabla \cdot (n \nabla \psi), \\ \frac{\partial \psi}{\partial t} &= \frac{1}{2}(\nabla \psi)^2 - \frac{e}{m}\varphi + \frac{\delta}{m}n^{2/3}, \\ \Delta \varphi &= \frac{4\pi e}{\varepsilon_\infty}(n - N_0) + \frac{4\pi\alpha}{\varepsilon_\infty} \nabla \cdot \mathbf{u}, \\ \frac{\partial^2 \mathbf{u}}{\partial t^2} &= -\omega_T^2 \mathbf{u} - \frac{\alpha}{\rho} \nabla \varphi, \end{aligned} \quad (3)$$

where $\delta=(3\pi^2)^{2/3}\hbar^2/2m$. It is easily seen that the system (3) is a set of the Euler equations for the following Lagrangian:

$$\begin{aligned} L = \int d^3r \left[\frac{1}{2}\rho\dot{\mathbf{u}}^2 - \frac{1}{2}\rho\omega_T^2\mathbf{u}^2 - \alpha \nabla \varphi \cdot \mathbf{u} + \frac{\varepsilon_\infty}{8\pi}(\nabla \varphi)^2 + mn\dot{\psi} \right. \\ \left. - \frac{1}{2}mn(\nabla \psi)^2 + e\varphi(n - N_0) - \frac{3}{5}\delta n^{5/3} \right]. \end{aligned}$$

Using the standard linearization procedure, which consists in a series expansion of $n=n_0+n_1+n_2+\dots$, $\psi=\psi_1+\psi_2+\dots$, $\varphi=\varphi_0+\varphi_1+\varphi_2+\dots$, and $\mathbf{u}=\mathbf{u}_1+\mathbf{u}_2+\dots$ in their deviations from equilibrium values, we obtain the following linear system of coupled equations:

$$\begin{aligned} \frac{\partial \psi_1}{\partial t} &= -\frac{e}{m}\varphi_1 + \frac{\beta^2}{n_0}n_1, \\ \frac{\partial n_1}{\partial t} &= \nabla \cdot (n_0 \nabla \psi_1), \\ \Delta \varphi_1 &= \frac{4\pi e}{\varepsilon_\infty}n_1 + \frac{4\pi\alpha}{\varepsilon_\infty} \nabla \cdot \mathbf{u}_1, \\ \frac{\partial^2 \mathbf{u}_1}{\partial t^2} &= -\omega_T^2 \mathbf{u}_1 - \frac{\alpha}{\rho} \nabla \varphi_1, \end{aligned} \quad (4)$$

as a first approximation. Here n_0 is the electron concentration and $\beta=(2\delta n_0^{2/3}/3m)^{1/2}$ is the speed of the propagation of the hydrodynamic disturbance in the electron gas. The Hamiltonian corresponding to Eqs. (4) is given by

$$\begin{aligned} H = \int d^3r \left[\frac{\rho\mathbf{u}_1^2}{2} + \frac{\rho\omega_T^2\mathbf{u}_1^2}{2} + \alpha \nabla \varphi_1 \cdot \mathbf{u}_1 - e\varphi_1 n_1 - \frac{\varepsilon_\infty(\nabla \varphi_1)^2}{8\pi} \right. \\ \left. + \frac{mn_0(\nabla \psi_1)^2}{2} + \frac{m\beta^2 n_1^2}{2n_0} \right]. \end{aligned} \quad (5)$$

Hereinafter the subscript 1 will be omitted for simplicity.

The solution of the system (4) with the appropriate boundary conditions allows the finding of the SPLP eigenmodes, their dispersion, and the self-consistent electric potential induced by the modes. For the program to be made, we considered Eqs. (4) in all regions of the heterostructure (Fig. 1) and solved them for the doped (d) and undoped (u) parts of the heterostructure, as well as for air (a). For matching the solutions, the following boundary conditions were used: an equality to zero of the normal component of hydrodynamic velocity, $d\psi_d/dz|_{z=0}=0$, and a continuity of the self-consistent electric potential, $\varphi_d|_{z=0}=\varphi_u|_{z=0}$, $\varphi_u|_{z=b}=\varphi_a|_{z=b}$, as well as the normal component of electric displacement, $\varepsilon_d(\omega)d\varphi_d/dz|_{z=0}=\varepsilon_u(\omega)d\varphi_u/dz|_{z=0}$, $\varepsilon_u(\omega)d\varphi_u/dz|_{z=b}=d\varphi_a/dz|_{z=b}$, where $\varepsilon_i(\omega)=\varepsilon_{i\infty}(\omega^2-\omega_{iL}^2)/(\omega^2-\omega_{iT}^2)$ for $i=d$ or u , and ω_{iL} are the limiting frequencies of longitudinal optical phonons. Analysis has shown that the SPLP modes occur near the interface between doped and undoped materials if the following inequality is satisfied:

$$\beta^2\Gamma_q^2 = \omega_p^2 \frac{\varepsilon_{d\infty}}{\varepsilon_d(\omega)} + \beta^2\mathbf{q}^2 - \omega^2 > 0, \quad (6)$$

where \mathbf{q} is the two-dimensional wave vector of the SPLP excitation and $\omega_p=\sqrt{4\pi n_0 e^2/\varepsilon_{d\infty} m}$ is the plasma frequency. Then we obtain that the SPLP modes have two branches, $\hbar\omega_{s\pm}(q)$, of the dispersion relation determined by the equation

$$\beta^2\Gamma_q(\Gamma_q + q) = \frac{\omega_p^2}{2} \frac{\varepsilon_{d\infty}}{\varepsilon_d(\omega)} \frac{2\varepsilon(\omega)}{\varepsilon(\omega) + \varepsilon_d(\omega)}, \quad (7)$$

where $\varepsilon(\omega)=\varepsilon_u(\omega)\eta_-(\omega)/\eta_+(\omega)$,

$$\eta_{\pm}(\omega) = 1 \pm \frac{\varepsilon_u(\omega) - 1}{\varepsilon_u(\omega) + 1} e^{-2qb}. \quad (8)$$

Figure 2 (left panel) illustrates the dispersion relation for the case when both the doped and undoped parts of the heterostructure are filled with the same material (GaAs). One can see that the branches $\hbar\omega_{s\pm}(q)$ have minima at the nonzero value of the wave vector $q_{d\pm}$. These minima result from the availability of the second interface (GaAs/air) between the mediums with essentially different dielectric constants. The depths, $\omega_{s\pm}(0)-\omega_{s\pm}(q_{d\pm})$, and positions $q_{d\pm}$ of the minima depend on the undoped layer thickness (b) (Fig. 3). Such points of the quasiparticle energy spectra, where $\text{grad}_{\mathbf{q}}\omega(\mathbf{q})=0$, are called critical points. In the case considered, since the functions $\omega_{s\pm}(q)$ are isotropic in the \mathbf{q} space, the critical points form circles with radii $q_{d\pm}$. The critical points $q_{d\pm}$ in the energy spectra result in the appearance of critical points $\hbar\omega_{d\pm}=\hbar\omega_{s\pm}(q_{d\pm})$ of the SPLP density of states,

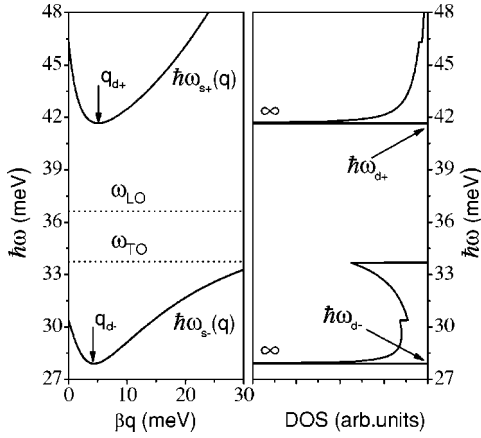


FIG. 2. Left: The dispersion branches $\hbar\omega_{s\pm}(q)$ for the SPLP modes in the double n -GaAs/GaAs heterostructure (Fig. 1). The concentration of free electrons equals $n_0 = 10^{18} \text{ cm}^{-3}$. The thickness of the undoped GaAs layer is 50 nm. Right: The density of states (DOS) corresponding to the SPLP branches. The symbol ∞ marks the critical points in which the DOS diverges as $(\hbar\omega - \hbar\omega_{d\pm})^{-1/2}$.

$$G_{s\pm}(\hbar\omega) = \int \frac{d\mathbf{q}}{(2\pi)^2} \delta[\hbar\omega - \hbar\omega_{s\pm}(q)]. \quad (9)$$

It should be emphasized that the critical points of this type are absent in the case of a single heterostructure.²⁸ This can be seen from Eq. (7) in the limiting case, $b \rightarrow \infty$. The SPLP density of states (DOS) corresponding to the dispersion branches $\hbar\omega_{s\pm}(q)$ plotted in Fig. 2 (left panel) is shown in the right panel of Fig. 2. Performing a simple analysis of Eq. (9), one can see that the DOS diverges as $(\hbar\omega - \hbar\omega_{d\pm})^{-1/2}$ at the critical points $\hbar\omega_{d\pm}$. Although this behavior of the DOS is typical of one-dimensional systems,³⁸ our result obtained for

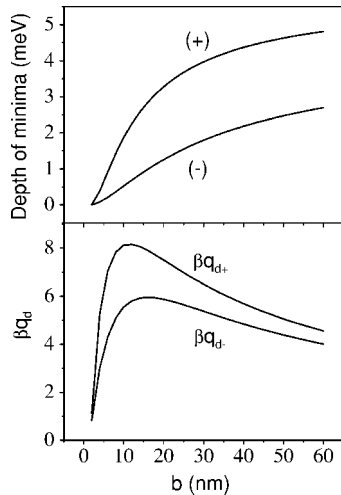


FIG. 3. Top: The depth of the minima in the high (+) and low (-) energy dispersion branches $\hbar\omega_{s\pm}(q)$ of the SPLP modes in the double n -GaAs/GaAs heterostructure (Fig. 1) as a function of the thickness (b) of the undoped GaAs layer. Bottom: The position of the minima as a function of the thickness (b) of the undoped GaAs layer. In both cases the concentration of free electrons equals $n_0 = 10^{18} \text{ cm}^{-3}$.

the two-dimensional problem is not surprising because the isotropy of the SPLP dispersion reduces the dimension of the system considered. The aforementioned characteristics of the DOS should be expressed in the SPLP-assisted processes.

The use of the solution of the system (4) for the secondary quantization of the fields involved in the Hamiltonian (5) is equivalent to an introduction of the SPLP excitations with the creation (annihilation) operators, $b_{\mathbf{q}j}^+(b_{\mathbf{q}j})$, where $j=+$ and $-$. As a result, the Hamiltonian (5) takes the form,

$$H = \sum_{\mathbf{q}j} \hbar\omega_{sj}(\mathbf{q})(b_{\mathbf{q}j}^+ b_{\mathbf{q}j} + 1/2),$$

and the self-consistent electric potential induced by the SPLP modes can be represented as

$$\varphi_s(\mathbf{r}) = \sum_{\mathbf{q},j} [\varphi_{\mathbf{q}j}(z)e^{i\mathbf{q}\cdot\mathbf{x}} b_{\mathbf{q}j} + \varphi_{\mathbf{q}j}^*(z)e^{-i\mathbf{q}\cdot\mathbf{x}} b_{\mathbf{q}j}^+], \quad (10)$$

where \mathbf{x} is the coordinate vector in the interface plain,

$$\varphi_{\mathbf{q}j}(z) = \begin{cases} \frac{\Gamma_q e^{qz} - q e^{\Gamma_q z}}{\Gamma_q - q} + \frac{q \varepsilon(\omega)(e^{qz} - e^{\Gamma_q z})}{\varepsilon_d(\omega)(\Gamma_q - q)}, & z \leq 0 \\ \frac{e^{-qz}}{\eta_+(\omega)} + \frac{[\eta_+(\omega) - 1]e^{qz}}{\eta_+(\omega)}, & 0 < z < b \\ \frac{2\varepsilon_u(\omega)}{\varepsilon_u(\omega) + 1} \frac{e^{-qz}}{\eta_+(\omega)}, & z > b, \end{cases} \quad (11)$$

$$\varphi_q = -\frac{4\pi e}{\varepsilon_d(\omega) + \varepsilon(\omega)} \left[\frac{\hbar\Gamma_q n_0}{L^2 q(2\Gamma_q + q)m\omega\sigma_s(\omega)} \right]^{1/2}, \quad (12)$$

$$\sigma_s(\omega) = 1 + \frac{(4\pi e)^2 n_0}{m(2\Gamma_q + q)\varepsilon_d^2(\omega)[\varepsilon_d(\omega) + \varepsilon(\omega)]^2} \times \left(\frac{\alpha_d^2 2\Gamma_q \varepsilon_d^2(\omega) + q[\varepsilon_d(\omega) + \varepsilon(\omega)]^2}{\rho_d (\omega^2 - \omega_{dT}^2)^2} + \frac{\alpha_u^2 2\Gamma_q \varepsilon_d^2(\omega)}{\rho_u (\omega^2 - \omega_{uT}^2)^2} \varpi_q \right), \quad (13)$$

$$\varpi_q = \frac{1}{\eta_+^2(\omega)} [1 - e^{-2qb} + [\eta_+(\omega) - 1]^2 (e^{2qb} - 1)]. \quad (14)$$

In Eqs. (11)–(14) ω equals $\omega_{s+}(q)$ or $\omega_{s-}(q)$ and L^2 is the normalization area.

Obviously, the coupling between the SPLP modes and any charged excitations, e.g., electrons and holes, can be expressed by the operator $e\varphi_s(\mathbf{r})$. This type of interaction corresponds to the SPLP-assisted light absorption, luminescence, and Raman scattering, as well as the intraband carrier relaxation. As an example, the relaxation process developing in the QD electronic subsystem will be considered in the next section.

III. INTRABAND RELAXATION RATES OF QUANTUM DOTS

The results described in the previous section allow one to calculate the intraband relaxation rates of QD electrons or holes due to the interaction with the doped part of the double heterostructure (Fig. 1) via the electric potential (10) induced by the SPLP modes. This coupling gives rise to the transitions between the initial (E_i) and final (E_f) states of the electron (hole) upon emission or absorption of the SPLP quanta. Supposing that the temperatures are relatively small, $\omega_{s\pm}(q)/k_B T \gg 1$, we can restrict our consideration to the relaxation processes with the emission of the SPLP modes.

The intraband relaxation rates can be calculated by different methods, e.g., in the framework of the Wigner-Weisskopf coupled-mode equation approach used for analysis of the phonon bottleneck in quantum dots.⁶ Instead, for simplicity's sake, we employ the Fermi golden-rule-based method which is commonly used for such types of calculations.^{5,14,17,18,21,23-25}

The rates of the intraband transitions as a function of the intraband QD level spacing $\Omega = (E_i - E_f)/\hbar$ are given by

$$W_s^{(f,i)} = \frac{2\pi}{\hbar^2} \sum_{\mathbf{q}j} | \langle i | e \varphi_{\mathbf{q}j}(z) e^{i\mathbf{q}x} | f \rangle |^2 e^{-2qa} \delta[\Omega - \omega_{sj}(q)], \quad (15)$$

where the origin of the coordinates is chosen at the QD position a . In the general case, the initial, final, or both QD states are degenerate in some quantum numbers which will be marked by primes in the equation below. To take into account this degeneration in Eq. (15), one should use the operation $Av_{f,i}$, implying averaging over the degenerate initial QD states $|i, i'\rangle$ and summation over the degenerate final QD states $|f, f'\rangle$. As a result we obtain the following expression for the intraband relaxation rate:

$$W_s^{(f,i)} = \frac{2\pi}{\hbar^2} \sum_{\mathbf{q}j} F_j^{(f,i)}(\mathbf{q}) e^{-2qa} \delta[\Omega - \omega_{sj}(q)], \quad (16)$$

where the function

$$F_j^{(f,i)}(\mathbf{q}) = Av_{f,i} | \langle i, i' | e \varphi_{\mathbf{q}j}(z) e^{i\mathbf{q}x} | f, f' \rangle |^2 \quad (17)$$

contains all information on QD parameters. Equation (16) is similar in its mathematical structure to the SPLP density of states [Eq. (9)]; hence, the relaxation rate will diverge at the DOS critical points. In order to avoid this problem, we replace the δ function in Eq. (16) by the Lorentzian

$$\delta[\Omega - \omega_{sj}(q)] \rightarrow \frac{1}{\pi} \frac{\gamma}{[\Omega - \omega_{sj}(q)]^2 + \gamma^2}, \quad (18)$$

where $\gamma = 1/2(\gamma_i + \gamma_f + \gamma_s) + \gamma_{pd}$ is the total dephasing rate of the transition between the initial and final QD states, γ_i , γ_f , and γ_s are the inverse lifetimes of electron (hole) states (i and f) and the SPLP excitations (s), and γ_{pd} is the pure dephasing rate. The phenomenological parameter γ in Eq. (18) is determined by the relaxation processes differing from SPLP-assisted relaxation.

Further analysis of the intraband carrier relaxation is possible only for a particular QD model. Let us consider a cy-

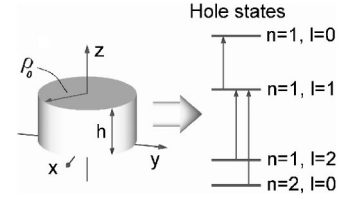


FIG. 4. The scheme of a cylindrical quantum dot. Several low energy hole states for the strong confinement regime are shown.

lindrical quantum dot (Fig. 4) frequently used for modeling real QD systems.³⁹⁻⁴¹ We will restrict ourselves to the case of the strong confinement regime, i.e., suppose that the height (h) and radius (ρ_0) of the QD are smaller than the exciton Bohr radius of QD bulk material. For definiteness' sake, we will consider the intraband hole relaxation. Similar results can be obtained for the electronic relaxation. The energy spectrum and wavefunctions of the hole states in a cylindrical QD, provided there is an infinite potential barrier, are given by

$$\Psi_{knl}(\mathbf{r}) = \sqrt{\frac{2}{\pi h \rho_0^2}} \frac{J_l(\xi_{ln} \rho / \rho_0)}{J_{l+1}(\xi_{ln})} \sin\left(\frac{\pi k}{h} z\right) e^{il\varphi}, \quad (19)$$

$$E_{knl} = \frac{\hbar^2}{2m_{QD}} \left(\frac{\pi^2 k^2}{h^2} + \frac{\xi_{ln}^2}{\rho_0^2} \right), \quad (20)$$

where $k=1, 2, 3, \dots$, ξ_{ln} is the n th zero of the Bessel function of the l th order [$J_l(\xi_{ln})=0$], and m_{QD} is the hole effective mass. The use of Eqs. (19) and (20) for calculating the function $F_j^{(f,i)}(\mathbf{q})$ gives the following result:

$$F_j^{(f,i)}(\mathbf{q}) = \frac{2e^2 \varphi_d^2 B(l_f)}{\eta_+^2(\omega)} [T_{k_f}^{k_i}(q) I_{k_f}^{k_i}(q) J_{l_f}^{l_i}(q)]^2, \quad (21)$$

where $B(l_f)=1$ for $l_f=0$, and $B(l_f)=2$ for other cases,

$$T_{k_f}^{k_i}(q) = (1 + (-1)^{k_f+k_i} [\eta_+(\omega) - 1]) e^{q(h+2a)},$$

$$I_{k_f}^{k_i}(q) = \frac{4\pi^2 q h [1 - (-1)^{k_f+k_i} e^{-qh}] k_f k_i}{[q^2 h^2 + \pi^2 (k_f - k_i)^2] [q^2 h^2 + \pi^2 (k_f + k_i)^2]}, \quad (22)$$

$$J_{l_f}^{l_i}(q) = 2 \int_0^1 dx x \frac{J_{l_f}(\xi_{l_f} x) J_{l_i}(\xi_{l_i} x) J_{l_f - l_i}(q \rho_0 x)}{J_{l_f+1}(\xi_{l_f}) J_{l_i+1}(\xi_{l_i})},$$

and $\omega = \omega_{sj}(q)$. Finally, the intraband relaxation rate of holes is given by

$$W_s^{(f,i)} = \sum_j \int_0^\infty \frac{dq}{\pi} \frac{B(l_f) m \Gamma_q \omega}{\hbar n_0 (2\Gamma_q + q) \sigma_s(\omega)} \frac{\gamma}{(\Omega - \omega)^2 + \gamma^2} \times \left[\frac{\varepsilon_{d\infty}}{\eta_+(\omega) [\varepsilon_d(\omega) + \varepsilon(\omega)]} \frac{\omega_p^2}{\omega} \right]^2 \times [T_{k_f}^{k_i}(q) I_{k_f}^{k_i}(q) J_{l_f}^{l_i}(q)]^2 e^{-2qa}, \quad (23)$$

where, as before, $\omega = \omega_{sj}(q)$.

In real quantum dots based on III-V semiconductors the hole energy spectra have complicated structures due to the

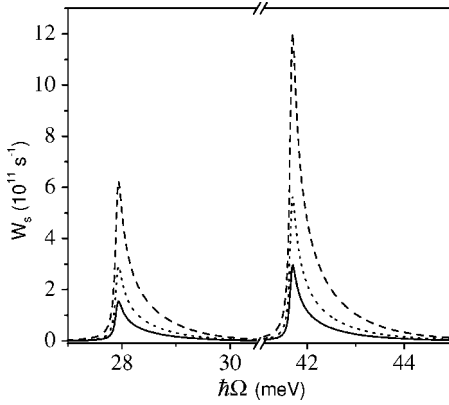


FIG. 5. The hole relaxation rates as a function of the level spacing Ω for three intraband transitions: the solid lines, $|2\rangle \rightarrow |1\rangle$; the dotted lines, $|3\rangle \rightarrow |2\rangle$; and the dashed lines, $|4\rangle \rightarrow |2\rangle$ (see the text). In calculations the following parameters were used: $a=40$ nm, $b=50$ nm, $n_0=10^{18}$ cm $^{-3}$, and $\gamma=0.05$ meV.

highly anisotropic valence band and the heavy and light hole state mixing.⁴² Moreover the built-in strain resulting from the lattice mismatch between the quantum dot and the matrix materials can essentially modify the hole spectra.⁴² Since we take an interest in the qualitative features of the relaxation process we neglect these effects and use the simple quantum dot model with single isotropic and parabolic valence bands corresponding, e.g., the heavy holes.

For illustration of the peculiarities of the intraband hole relaxation in the double heterostructure (Fig. 1) let us consider the InAs cylindrical QD with a fixed height, $h=5$ nm, and restrict ourselves to several low-energy hole states with the quantum number $k=1$: $|1\rangle=|n=1, l=0\rangle$, $|2\rangle=|n=1, l=1\rangle$, $|3\rangle=|n=1, l=2\rangle$, and $|4\rangle=|n=2, l=0\rangle$ (see Fig. 4). In all calculations the effective mass ($m_{QD}=0.41 m_0$) of heavy holes for the InAs QD has been used. The qualitatively same results are obtained if using the effective mass values in the range of $0.43-0.35 m_0$ that are reasonable for InAs.⁴³ A relation of $\rho_0=\sqrt{\hbar(\xi_i^2-\xi_j^2)}/(2m_{QD}^2\Omega)$ (where $i=2, j=1$ or $i=3, j=2$ or $i=4, j=2$) between the QD radius and Ω was employed for taking into account the variations of the level spacing energy with the QD size. If the QD size is fixed and the level spacing energy is varied by other means, e.g., by the arbitrary changing of Ω in the equations, the qualitatively same spectra of the relaxation rates have been obtained. Figure 5 shows the hole relaxation rates [Eq. (23)] as a function of the level spacing Ω for transitions $|2\rangle \rightarrow |1\rangle$, $|3\rangle \rightarrow |2\rangle$, and $|4\rangle \rightarrow |2\rangle$ in the quantum dot embedded in the undoped GaAs part of the heterostructure at a distance $a=40$ nm from its doped GaAs part. One can see that two relaxation windows corresponding to the high $[\omega_{s+}(q)]$ and low $[\omega_{s-}(q)]$ energy dispersion branches of the SPLP modes are opened. The relaxation rates are sufficiently large and are of the same order of magnitude for all three transitions. In calculations we assume that the undoped layer thickness (b) and the transition dephasing rates (γ) are equal to 50 nm and 0.05 meV, respectively. Figure 6 shows the relaxation rate spectra for different b for the $|2\rangle \rightarrow |1\rangle$ transition and the same spectrum for a single heterostructure.

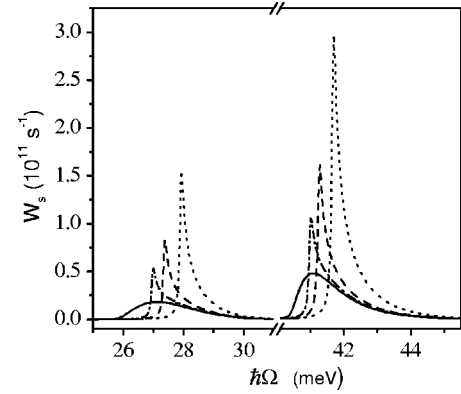


FIG. 6. The hole relaxation rates as a function of the level spacing Ω of the intraband transition $|2\rangle \rightarrow |1\rangle$ for different undoped layer thicknesses (b): the dotted lines, $b=50$ nm; the dashed lines, $b=80$ nm; and the dash-dotted lines, $b=120$ nm. The solid lines show the corresponding relaxation rates for a single heterostructure. In calculations the following parameters were used: $a=40$ nm, $n_0=10^{18}$ cm $^{-3}$, and $\gamma=0.05$ meV.

Three main distinctions between the double and single heterostructures are clearly seen. The existence of the critical points of the SPLP DOS for the double heterostructure results in a significant enhancement of the intraband relaxation rates compared with the single heterostructure. Furthermore, the narrowing of the spectral widths of the relaxation windows takes place. Finally, the spectral positions of the relaxation windows are shifted toward higher energies with decreasing of the undoped layer thickness. Certainly, the enhancement value strongly depends on the transition dephasing rate (γ). Although the reliable data on γ are lacking, we can estimate the lower limit of γ . In accordance with the results obtained by several research groups,⁴⁴⁻⁴⁸ the electronic (hole) dephasing rates in QDs at low temperatures vary from several μ eV to several tens of μ eV. Therefore, in our calculations, a γ value of 50 μ eV was used. On the other hand, the inverse lifetime (γ_s) of the SPLP modes contributes to γ additively. Its value is unknown *a priori*. In order to

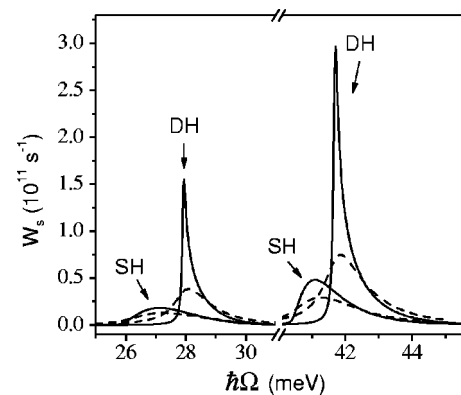


FIG. 7. Hole relaxation rates as a function of the level spacing Ω of the intraband transition $|2\rangle \rightarrow |1\rangle$ for different dephasing rates (γ): the solid lines, $\gamma=0.05$ meV; the dashed lines, $\gamma=0.5$ meV. The symbols SH and DH indicate single and double heterostructures, respectively. In calculations the following parameters were used: $a=40$ nm, $b=50$ nm, and $n_0=10^{18}$ cm $^{-3}$.

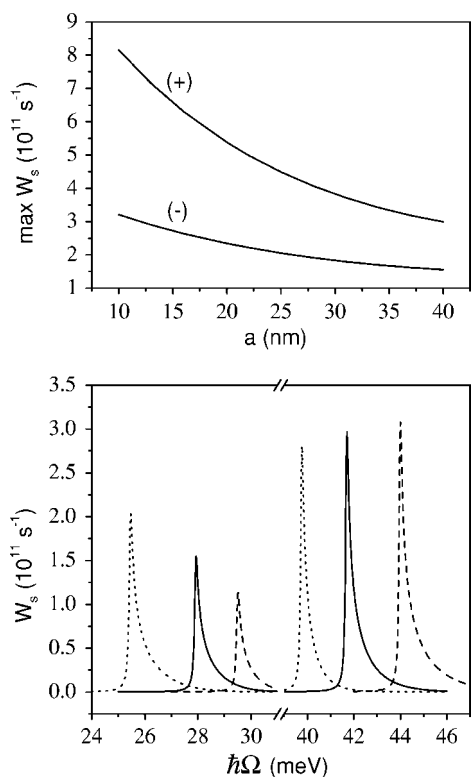


FIG. 8. Top: The maximum hole relaxation rates for the transition $|2\rangle \rightarrow |1\rangle$ as a function of the distance (a) between the QD and the doped substrate. Signs (+) and (-) correspond to the high and low energy relaxation windows, respectively; $b=50$ nm, $n_0=10^{18}$ cm $^{-3}$, and $\gamma=0.05$ meV. Bottom: The hole relaxation rates as a function of the level spacing Ω of the intraband transition $|2\rangle \rightarrow |1\rangle$ for different free carrier concentrations (n_0): the dotted lines, $n_0=0.75 \times 10^{18}$ cm $^{-3}$; the solid lines, $n_0=10^{18}$ cm $^{-3}$; and the dashed lines, $n_0=1.25 \times 10^{18}$ cm $^{-3}$. In calculations the following parameters were used: $a=40$ nm, $b=50$ nm, and $\gamma=0.05$ meV.

clarify this problem, we calculated the hole intraband relaxation rates with a γ value of $500 \mu\text{eV}$, assuming that γ was determined by γ_s (see Fig. 7).

One can see that even for this case the enhancement of the intraband relaxation rates in the double heterostructure is about three times higher than in the single heterostructure. Notwithstanding significant differences, the intraband relaxation rates in double heterostructures exhibit the $n_0(a)$ dependence similar to that for a single heterostructure²⁸ (see Fig. 8). Figure 8 shows that the spectral positions of the relaxation windows are changed with n_0 and the relaxation rates increase with decreasing a .

Our model proposes that the influence of the carriers generated in quantum dots on the SPLP spectrum of the doped

heterostructure is negligible. It takes place at a small number of carriers inside the dot and the low concentration of the dots embedded in the heterostructure. In the opposite limit, the influence may result in a renormalization of the SPLP spectrum. We did not also consider the effects which are characteristic for real quantum dot heterostructures: the shape and/or strain dependence of the quantum dot electronic structure and the dipole momenta of the transitions. Although these limitations do not affect the qualitative conclusions of our work, they should be considered in the quantitative analysis of the intraband relaxation rate in real quantum-dot systems in doped heterostructures. Finally, the coupled plasmon-acoustic-phonon modes can also take place in the semiconductor system under study due to the piezoelectric effect. Evidently their coupling with the quantum-dot carriers is also possible via an interaction like that described above. The study of this interesting problem is now in progress. It is worth noting that relaxation processes caused by this mechanism do not interfere with those considered in this paper since energies of the plasmon-acoustic-phonon modes are in other ranges than the SPLP ones.

IV. CONCLUSION

It has been shown that the SPLP density of states inherent in a doped semiconductor is essentially modified when a layer of undoped material of finite thickness is grown on the semiconductor. Specifically, the critical points of the SPLP DOS arise with their positions depending on the layer thickness. The presence of the critical points results in the enhancement of the relaxation processes involving the SPLP in the probe embedded in the undoped layer. Using the quantum dot as a probe, we showed that the intraband relaxation in QD is enhanced for the thin layer compared with that for the macroscopic layer. In other words, a “dielectric confinement” of the SPLP takes place in these kinds of layered structures. The actual values of relaxation rates in real systems can differ from those calculated by us. This fact, however, does not affect our qualitative conclusions. Obviously, these characteristic features of the SPLP DOS are important for nanostructure-based applications, where the QD layer located at distances of tens or several tens of nanometers from the $n(p)$ -doped elements of heterostructures and covered with a thin cup layer are widely used. The concentration, distance, and layer thickness dependencies of the relaxation rates offer wide opportunities for the manipulation of QD electronic dynamics in doped heterostructures.

We would like to thank Professor U. Woggon for valuable discussions. This work was partially supported by the INTAS Program (project Grant Nos. 01-2100 and 01-2331).

*Email address: a_v_fedorov@inbox.ru

¹L. Guo, E. Leobandung, and S. Chou, *Science* **275**, 649 (1997).

²T. Itakura and Y. Tokura, *Phys. Rev. B* **67**, 195320 (2003).

³K. Yano, T. Ishii, T. Sano, T. Mine, F. Murai, T. Hashimoto, T.

Koboyashi, T. Kure, and K. Seki, *Proc. IEEE* **87**, 633 (1999).

⁴M. Dutta and M. A. Stroschio, *Advances in Semiconductor Lasers and Applications to Optoelectronics* (World Scientific, Singapore, 2000).

- ⁵X.-Q. Li and Y. Arakawa, Phys. Rev. B **57**, 12 285 (1998).
- ⁶X.-Q. Li, H. Nakayama, and Y. Arakawa, Phys. Rev. B **59**, 5069 (1999).
- ⁷F. Gindele, K. Hild, W. Langbain, and U. Woggon, Phys. Rev. B **60**, R2157 (1999).
- ⁸A. V. Baranov, V. Davydov, H.-W. Ren, S. Sugou, and Y. Masumoto, J. Lumin. **87–89**, 503 (2000).
- ⁹I. V. Ignatiev, I. E. Kozin, S. V. Nair, H.-W. Ren, S. Sugou, and Y. Masumoto, Phys. Rev. B **61**, 15 633 (2000).
- ¹⁰I. V. Ignatiev, I. E. Kozin, V. G. Davydov, S. V. Nair, J.-S. Lee, H.-W. Ren, S. Sugou, and Y. Masumoto, Phys. Rev. B **63**, 075316 (2001).
- ¹¹P. A. Knipp and T. L. Reinecke, Phys. Rev. B **46**, 10 310 (1992).
- ¹²G. Biese, C. Schüller, K. Keller, C. Steinebach, D. Heitmann, P. Grambow, and K. Eberl, Phys. Rev. B **53**, 9565 (1996).
- ¹³S. Zanier, Y. Guldner, J. P. Vieren, G. Faini, E. Cambril, and Y. Campidelli, Phys. Rev. B **57**, 1664 (1998).
- ¹⁴T. Inoshita and H. Sakaki, Phys. Rev. B **46**, 7260 (1992).
- ¹⁵R. Heitz, M. Veit, N. N. Ledentsov, A. Hoffman, D. Bimberg, V. M. Ustinov, P. S. Kop'ev, and Z. I. Alferov, Phys. Rev. B **56**, 10 435 (1997).
- ¹⁶P. C. Sersel, Phys. Rev. B **51**, 14 532 (1995).
- ¹⁷D. F. Schroeter, D. F. Griffiths, and P. C. Sersel, Phys. Rev. B **54**, 1486 (1996).
- ¹⁸X.-Q. Li and Y. Arakawa, Phys. Rev. B **56**, 10 423 (1997).
- ¹⁹O. Verzelen, R. Ferreira, and G. Bastard, Phys. Rev. B **62**, R4809 (2000).
- ²⁰S. Sauvage, P. Boucaud, R. Lobo, F. Bras, G. Fishman, R. Prazeres, F. Glotin, J. Ortega, and J.-M. Gerard, Phys. Rev. Lett. **88**, 177402 (2002).
- ²¹U. Bockelmann and T. Egeler, Phys. Rev. B **46**, 15 574 (1992).
- ²²A. L. Efros, V. A. Kharchenko, and M. Rosen, Solid State Commun. **93**, 281 (1995).
- ²³U. Bockelmann and G. Bastard, Phys. Rev. B **42**, 8947 (1990).
- ²⁴H. Benisty, Phys. Rev. B **51**, 13 281 (1995).
- ²⁵A. V. Fedorov, A. V. Baranov, and Y. Masumoto, Solid State Commun. **122**, 139 (2002).
- ²⁶A. V. Uskov, K. Nishi, and R. Lang, Appl. Phys. Lett. **74**, 3081 (1999).
- ²⁷A. V. Baranov, A. V. Fedorov, I. D. Rukhlenko, and Y. Masumoto, Phys. Rev. B **68**, 205318 (2003).
- ²⁸A. V. Fedorov, A. V. Baranov, I. D. Rukhlenko, and Y. Masumoto, Solid State Commun. **128**, 219 (2003).
- ²⁹M. G. Cottam and D. R. Tilley, *Introduction to Surface and Superlattice Excitations* (Cambridge University Press, Cambridge, U.K., 1989).
- ³⁰R. H. Ritchie and R. E. Wilems, Phys. Rev. **178**, 372 (1969).
- ³¹G. Barton, Rep. Prog. Phys. **42**, 963 (1979).
- ³²J. Heinrichs, Phys. Rev. B **7**, 3487 (1973).
- ³³I. V. Tokatly and O. Pankratov, Phys. Rev. B **62**, 2759 (2000).
- ³⁴L. Kleinman, Phys. Rev. B **7**, 2288 (1973).
- ³⁵J. Dempsey and B. I. Halperin, Phys. Rev. B **45**, 1719 (1992).
- ³⁶E. Zaremba and H. C. Tso, Phys. Rev. B **49**, 8147 (1994).
- ³⁷H. Sun and K. Yu, Phys. Rev. B **61**, 16 174 (2000).
- ³⁸F. Bassani and G. P. Parravicini, *Electronic States and Optical Transitions in Solids* (Pergamon Press, London, 1975).
- ³⁹S. L. Goff and B. Stébé, Phys. Rev. B **47**, 1383 (1993).
- ⁴⁰J. Song and S. E. Ulloa, Phys. Rev. B **52**, 9015 (1995).
- ⁴¹P. Matagne and J.-P. Leburton, Phys. Rev. B **65**, 235323 (2003).
- ⁴²D. Bimberg, M. Grundmann, and N. N. Ledentsov, *Quantum Dot Heterostructures* (Wiley, New York, 1999).
- ⁴³*Semiconductors*, edited by O. Madelung and M. Schultz, Landolt-Börnstein, New Series, Group III, Vol. 22, Pt. A (Springer, Berlin, 1987).
- ⁴⁴D. Gammon, E. Snow, E. Shanabrook, D. Katzer, and D. Park, Science **273**, 87 (1996).
- ⁴⁵L. Besombes, K. Kheng, L. Marshal, and H. Mariette, Phys. Rev. B **63**, 155307 (2001).
- ⁴⁶P. Borri, W. Langbein, U. Woggon, R. Sellin, D. Ouyang, and D. Bimberg, Phys. Rev. Lett. **87**, 157401 (2001).
- ⁴⁷M. Bayer and A. Forchel, Phys. Rev. B **65**, 041308 (2002).
- ⁴⁸A. V. Baranov, V. Davydov, A. V. Fedorov, M. Ikezawa, H.-W. Ren, S. Sugou, and Y. Masumoto, Phys. Rev. B **66**, 075326 (2002).